Precambrian Research xxx (2014) xxx–xxx

Contents lists available at ScienceDirect

Precambrian Research

journal homepage: www.elsevier.com/locate/precamres

The four Neoproterozoic glaciations of southern Namibia and their detrital zircon record: The fingerprints of four crustal growth events during two supercontinent cycles

Mandy Hofmann[c,*], Ulf Linnemann[a], Karl-Heinz Hoffmann[b], Gerard Germs[c], Axel Gerdes[d,e], Linda Marko[d], Katja Eckelmann[a], Andreas Gärtner[a], Rita Krause[a]

[a] *Senckenberg Naturhistorische Sammlungen Dresden, Museum fuer Mineralogie und Geologie, Sektion Geochronologie, Koenigsbruecker Landstrasse 159, D-01109 Dresden, Germany*
[b] *Geological Survey of Namibia, 1 Aviation Road, P.O. Box 2168, Windhoek, Namibia*
[c] *Private Bag X607, Oudtshoorn 6620, South Africa*
[d] *Goethe Universität Frankfurt, Institut für Geowissenschaften, Mineralogie, Altenhoeferallee 1, D-60438 Frankfurt, Germany*
[e] *Department of Earth Sciences, Stellenbosch University, Private Bag X1, Matieland 7602, South Africa*

ARTICLE INFO

Article history:
Received 25 April 2014
Received in revised form 1 July 2014
Accepted 31 July 2014
Available online xxx

Keywords:
Namibia
Kaigas
Sturtian
Marinoan
Vingerbreek
Kalahari Craton

ABSTRACT

The transition from supercontinent Rodinia to Gondwana took place in the Neoproterozoic. The western margin of the Kalahari Craton in southern Namibia underwent rifting at c. 750 Ma, caused by the break-up of Rodinia, followed by drift-events and ongoing sedimentation throughout the Cryogenian (at least from 750 to 630 Ma) in Namibia. These sediments comprise at least three different deposits of glacio-marine diamictites (Kaigas at c. 750–720 Ma, Sturtian at c. 716 Ma and Marinoan at c. 635 Ma). The Ediacaran is characterised by collision during the assembly of Gondwana and includes a fourth glacial deposit (post-Gaskiers Vingerbreek glaciation at c. 547 Ma). This study presents more than 1050 single zircon grain U–Pb analyses of different diamictite horizons from southern Namibia and discusses their correlation. For all samples from sediments related to the Kaigas, Sturtian and Marinoan glacial events, the youngest obtained zircon ages were at c. 1.0 Ga, making differentiation by the maximum age of sedimentation impossible. But a correlation was still possible by using the complete detrital zircon U–Pb age patterns, with a significant change in the relative abundance of concordant Mesoproterozoic to Paleoproterozoic zircons. This P/M ratio seems to be a good tool to distinguish the Cryogenian diamictites (Marinoan: P/M < 0.4, Sturtian: 0.4 < P/M < 10, Kaigas: P/M > 10). Although all the observed ages from the detrital zircons can be explained by derivation of local material, none of our samples correspond to the Cryogenian rifting events in southern Namibia. Therefore the source area cannot be local and more probably is located in the east of the studied areas. The constancy of the main U–Pb ages suggests a constant sediment supply direction throughout the Cryogenian. The same age populations occurring in the Ediacaran Aar Member indicate the same sediment transport direction from the east, but with an increased proportion of zircon grains older than 2.2 Ga. This marks a transition to the unconformably overlying Vingerbreek (post-Gaskiers) diamictite horizons, which show a significant change in the age spectra. Probably due to mixed input from the east (Kalahari Craton) and from the west (Gariep Belt), the Vingerbreek diamictites show a wider range of zircon ages with youngest ages at c. 590 Ma. This time is characterised by collision events and the Gondwana formation. The Hf isotope record shows that the only input of juvenile material in our samples occurred in the Mesoproterozoic during the Namaqua Natal Orogeny (formation of the Namaqua Belt). In total, four Archaean to Proterozoic crustal growth events are recognised in the western part of the Kalahari Craton: (1) Meso- to Paleoarchean (c. 3.42–2.8 Ga), (2) lower Paleoproterozoic to Neoarchaean (c. 2.8–2.27 Ga), (3) lower to upper Paleoproterozoic (c. 2.27–1.7 Ga) and (3) Mesoproterozoic (c. 1.6–1.0 Ga).

* Corresponding author. Tel.: +49 351 795841 4419.
E-mail address: mandy.hofmann@senckenberg.de (M. Hofmann).

http://dx.doi.org/10.1016/j.precamres.2014.07.021
0301-9268/

1. Introduction

The middle to upper Neoproterozoic is characterised by the break-up of the supercontinent Rodinia and the assembly of Gondwana. This period includes various assumed occurrences of global or near-global glaciations. Of them, the Marinoan Snowball-Earth glaciation at c. 635–630 Ma is the most important and best constrained one (term after Mawson and Sprigg, 1950; originally for glacial sediments in South Australia; exact age for Namibia 635.5 ± 1.2 Ma according to Hoffmann et al., 2004). A second and older glaciation between c. 720 and 660 Ma (Shields-Zhou et al., 2012) is known as the Sturtian glacial event. An exact age was defined in Canada at c. 716.5 Ma according to McDonald et al. (2010a) while the term was originally derived from glacial deposits of the Sturt River Gorge in South Australia.

In addition to them, there is evidence for at least three more glacial events with unknown but possibly global extent: (i) The Kaigas glaciation at c. 750–720 Ma with an indirect age older than 741 ± 6 Ma from Namibia according to Frimmel et al. (1996), (ii) the Gaskiers glaciation at c. 580–582 Ma (exact age of 580 ± 1 Ma has been reported by Bowring et al. (2003) from Newfoundland) which is not known in southern Namibia, and (iii) the post-Gaskiers Vingerbreek glaciation at c. 547 Ma (Germs and Gaucher, 2012). Southern Namibia comprises at least four glacial deposits, although correlations were difficult due to changing stratigraphic columns and formation names.

Present day Namibia contains parts of the Kalahari Craton (S) and the Congo Craton (N). The first one comprises two units of Archaean crust: the Zimbabwe Craton (N) and the Kaapvaal Craton (S) with the Archaean to Paleoproterozoic Limpopo Belt in between (Fig. 1). This belt is interpreted as an exotic crustal block that probably got caught between the Zimbabwe and Kaapvaal Cratons during a 2.7–2.6 Ga collision (Begg et al., 2009). Both of the latter mentioned Archaean to Paleoproterozoic cores grew mainly along their NW margins (present day coordinates) in the Paleoproterozoic. This Mesoproterozoic "Proto-Kalahari Craton" (marked by the red dashed line in Fig. 1) was influenced by intense tectonic activity along all margins forming the Kalahari Craton as in its present extent (Jacobs et al., 2008). The southern and eastern margins of this craton are more or less equal to the Namaqua-Natal Belt. This major continuous belt of mainly high-grade rocks is a continental arc that evolved during accretion prior to continent-continent collision at c. 1.2–1.0 Ga and is associated with the formation of supercontinent Rodinia. According to Evans (2009), Jacobs et al. (2008) and others the Namaqua-Natal Belt comprises the remnants of a collision orogen evolved from the Kalahari-Australia/Mawsonland continent-continent collision. Simultaneously to this collision the Kalahari Craton was influenced by intra-plate magmatism, represented by the ca 1.11 Ga Umkondo-Borg Large Igneous Province (Jacobs et al., 2008).

In general, the Kalahari Craton is surrounded by a series of Neoproterozoic to Early Paleozoic (650–450 Ma) orogenic mobile belts ("Pan-African" in the broadest sense), such as Zambezi, Saldania, Gariep and Damara Belts (Fig. 1), which evolved through different phases of intra-continental rifting, continental break-up, spreading, plate motion reversal, subduction and finally continental collision (Frimmel et al., 2011; Jacobs et al., 2008). Parts of the Kalahari Craton were involved in at least two supercontinental cycles that resulted in the formation and dispersion of Rodinia and Gondwana. According to Jacobs et al. (2008) parts of the Kalahari Craton are also exposed in East- and West-Antarctica, in the Falkland Islands and possibly in South America, with all of them reflecting collision events with adjacent cratons.

As a supercontinent formation is not a stable construct, first rift-related structures in the western Kalahari Craton occurred already in the early Cryogenian at 800–750 Ma (Gaucher et al., 2010),

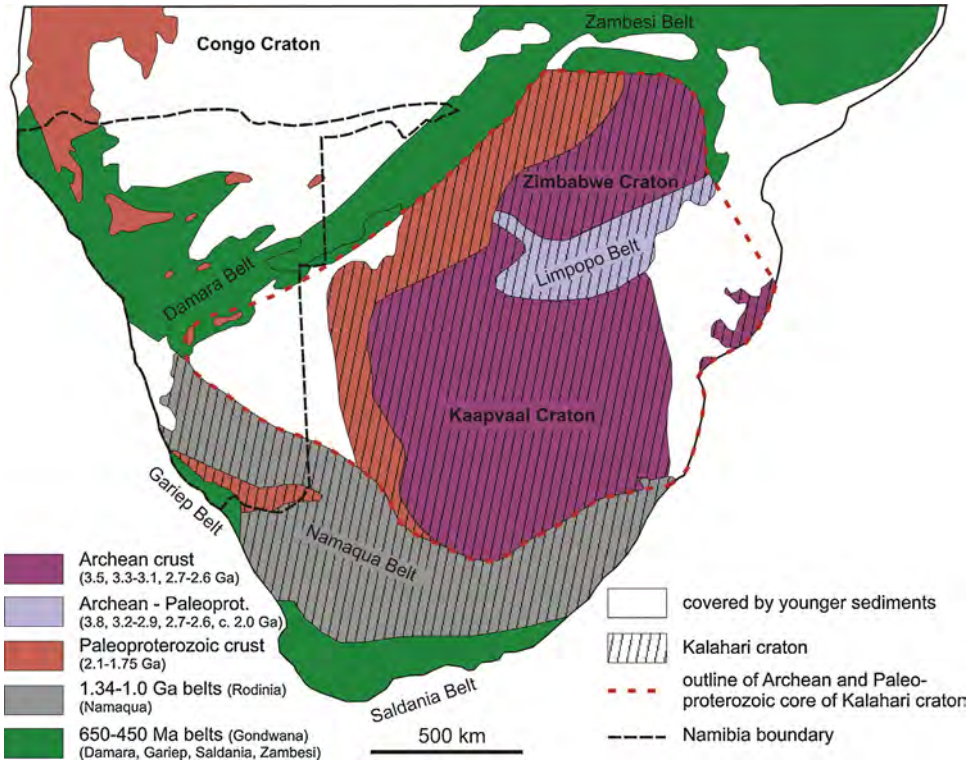

Fig. 1. Constitution of the Kalahari Craton and surrounding areas in southern Africa (from Hofmann et al., 2013; simplified after Jacobs et al., 2008). The Archaean to Paleoproterozoic core of the craton is completely surrounded by upper Neoproterozoic to lower Paleoproterozoic mobile belts, such as the Damara, Gariep and Saldania Belt. The Namaqua Belt is a result of the assembly of Rodinia supercontinent. Younger mobile belts are related to the assembly of Gondwana. Ages based on Jacobs et al. (2008) and Trompette (1994).

Please cite this article in press as: Hofmann, M., et al., The four Neoproterozoic glaciations of southern Namibia and their detrital zircon record: The fingerprints of four crustal growth events during two supercontinent cycles. Precambrian Res. (2014), http://dx.doi.org/10.1016/j.precamres.2014.07.021

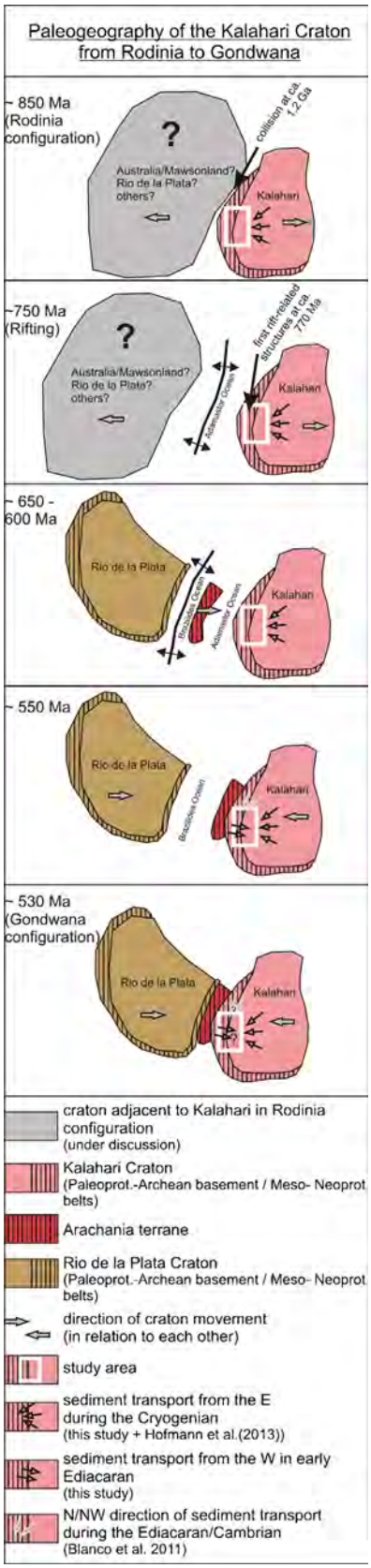

Fig. 2. Paleogeography of the Kalahari craton in the Neoproterozoic from Rodinia dispersal to Gondwana assembly (sketches slightly modified after Hofmann et al. (2013)). The size of cratons is not to scale. Cryogenian rift events are due to Rodinia break-up. Juxtaposition of Kalahari with Australia/Mawsonland, Rio de la Plata or another craton is still under discussion in the literature and therefore differs from author to author (e.g. Pisarevsky et al. (2003), Evans (2009), Li et al. (2008), Frimmel et al. (2011)). Location of the study area in southern Namibia is given as white rectangle. Sediment transport is considered to have been from the E/SE during the Cryogenian, providing detrital material directly from the Kalahari Craton. This changed in the early Ediacaran to a mixing of sediments from the east with input from the west (Hofmann et al. (2013) and results of this study). According to Blanco et al. (2011) main sediment input during the Ediacaran to Cambrian was from the N/NW.

indicating the initial break-up of Rodinia. Gaucher et al. (2010) termed this the "early Cryogenian rifting", which was followed by a second rifting event in the early Ediacaran at 630–600 Ma. Such Rodinia break-up structures are best preserved along the W, SW and NW margins of the Kalahari Craton, where there are rift sediments and volcanic rocks at 800–750 Ma (represented e.g. by the Rosh Pinah Fm in southern Namibia). According to Jacobs et al. (2008) the Kalahari Craton drifted away from Rodinia at c. 700 Ma.

Deposition of Cryogenian and Ediacaran tillites has been accompanied by rifting events that represent the initial Rodinia break-up. These events are interpreted to indicate the first drift-off of the Kalahari Craton from Australia/Mawsonland (according to Evans, 2009, Pisarevsky et al., 2003, and others) or the rifting between the Rio de la Plata Craton and the Kalahari Craton, as it is the favoured model by Frimmel et al. (2011) and Gaucher et al. (2010). For further discussion of this issue see also Hofmann et al. (2013). Cryogenian rifting events resulted in the opening of the Adamastor Ocean along the western margin of the Kalahari Craton. With respect to Gaucher et al. (2010) rift-related magmatism along the Kalahari Craton started already at about 830 Ma and lasted until c. 740 Ma. The closure of the Adamastor Ocean in Neoproterozoic times was a result of the approaching Kalahari and Rio de la Plata Cratons and therefore was part of the Gondwana formation (Fig. 2).

The basement of the area close to the Gariep Belt in southern Namibia (see Figs. 1 and 3) contains intrusive rocks of the Vioolsdrif Suite dated at 1.9–1.7 Ga and the 2.0 Ga old Orange River Group (Frimmel et al., 2011). The first one includes the Namuskluft section's basement located near the camp ground Namuskluft east of Rosh Pinah in southern Namibia. These rocks are dated at c. 1.9 Ga according to Hofmann et al. (2013). In addition to this, southern Namibia is characterised by high grade gneisses and felsic intrusions of the Namaqua Province (Fig. 3), containing e.g. arc-related c. 1.15 Ga granitoids (Bushmanland Terrane, South Africa) and supra-crustal units. Metamorphism of these units and intrusion of granites occurred between 1.08 and 1.03 Ga (Frimmel et al., 2011).

Younger, rift-related ages are known from the granitoids of the Richtersveld Suite, that document a first evidence of crustal thinning before the Rodinia break-up, and show three pulses of magmatism at 837 ± 2 Ma, 801 ± 8 Ma and 771 ± 6 Ma (Frimmel et al., 2011). This range of mainly felsic intrusions is arranged in a "line", starting at Richtersveld in South Africa and continuing towards NE direction to southern Namibia. They intruded the low-grade metamorphosed granitoids of the 1.9–1.7 Ga old Vioolsdrif Granite Suite and metavolcanic rocks of the 2.0 Ga old Orange River Group (Frimmel, 2008). The youngest intrusions linked to the three magmatic pulses of the Richtersveld Suite (771 ± 6 Ma) directly underlie the oldest sedimentary rocks of the Gariep Supergroup. Therefore, they determine the maximum age for beginning of Neoproterozoic sedimentation within the Gariep Basin. Ongoing break-up of Rodinia led to syn-rift magmatism that is exemplarily represented by the predominantly felsic volcanic rocks of the Rosh Pinah Fm, cropping out north of the town of Rosh Pinah. Due to thrusting and isolation, the stratigraphic position of this formation is not always clear, but it underlies the Sturtian diamictite horizon. The U–Pb single zircon age of 741 ± 6 Ma of a rhyolite of the Rosh Pinah Fm (Frimmel, 2008) gives a more accurate maximum age for the commencing of the sedimentation in this area. All rift-related igneous rocks show a within-plate geochemistry and

Please cite this article in press as: Hofmann, M., et al., The four Neoproterozoic glaciations of southern Namibia and their detrital zircon record: The fingerprints of four crustal growth events during two supercontinent cycles. Precambrian Res. (2014), http://dx.doi.org/10.1016/j.precamres.2014.07.021

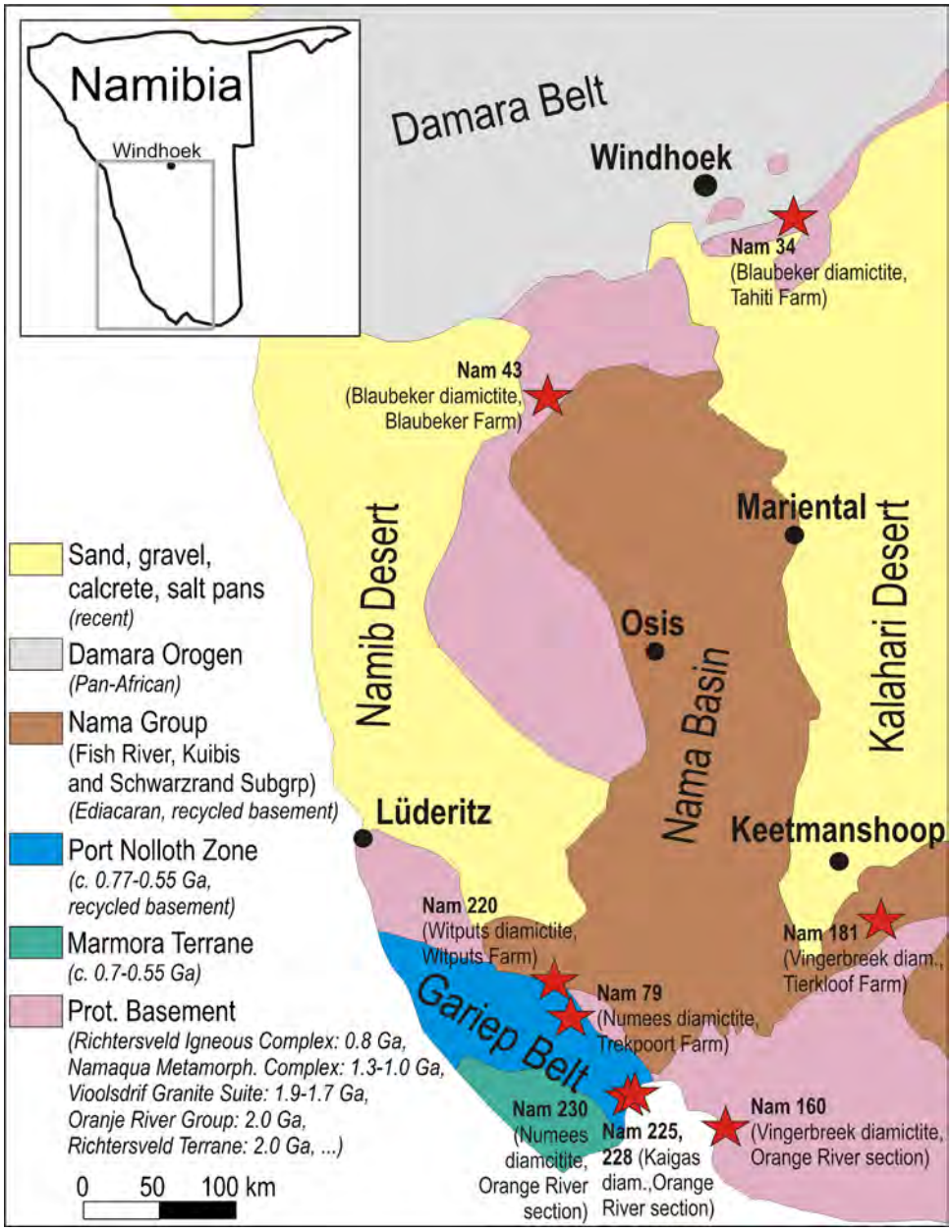

Fig. 3. Major geological units of southern Namibia (map extracted from "Simplified Geological Map of Namibia", Geol. Survey of Namibia, 1980). Sampling points of all nine samples presented in this study are given by red stars. Ages of the different units according to Frimmel (2008).

absence of flood basalts, which is typical for a non-volcanic margin (Jacobs et al., 2008 and references therein). The syn-rift magmatism has been followed by a syn-drift magmatism, documented by mafic units within the Marmora Terrane at c. 650–600 Ma (Frimmel, 2008). This corresponds to the beginning of Gondwana amalgamation (Pan-Africa events).

2. The samples

In this article, we present the detrital zircon records of nine diamictites of southern Namibia and their possible correlation. The sample points are shown in Figs. 3 and 4, the stratigraphic correlation is given in Fig. 5.

The samples from the Witputs Farm, Trekpoort Farm and from along the Orange River are situated within the Gariep Belt. Two Blaubeker diamictites represent the pre-Nama successions south of Windhoek and south of the Damara Belt. Two Vingerbreek diamictites belong to the Nama Group south of the Osis ridge (Fig. 3).

2.1. Blaubeker and Tahiti Farm (the Blaubeker diamictite)

We sampled two Blaubeker diamictites from different locations (see Figs. 3 and 4E and F). One of them has been taken at the eponymous Blaubeker Farm at S 23°53′37.1″, E 16°28′42.8″, Alt. 1629 m, ±4 m (Nam 43). The other sample has been taken at the Tahiti Farm at S 22°57′21.7″, E 18°43′34.3″, Alt. 1330 m, ±5 m (Nam 34).

The Blaubeker formation marks the base of the Witvlei Group and overlies Kamtsas quartzites (Fig. 5). Fig. 4E and F shows the appearance of the two Blaubeker diamictite samples. In both cases we analysed the sandy matrix. The diamictites are sheared and contain facetted pebbles and dropstones. In both cases we analysed the sandy matrix.

Please cite this article in press as: Hofmann, M., et al., The four Neoproterozoic glaciations of southern Namibia and their detrital zircon record: The fingerprints of four crustal growth events during two supercontinent cycles. Precambrian Res. (2014), http://dx.doi.org/10.1016/j.precamres.2014.07.021

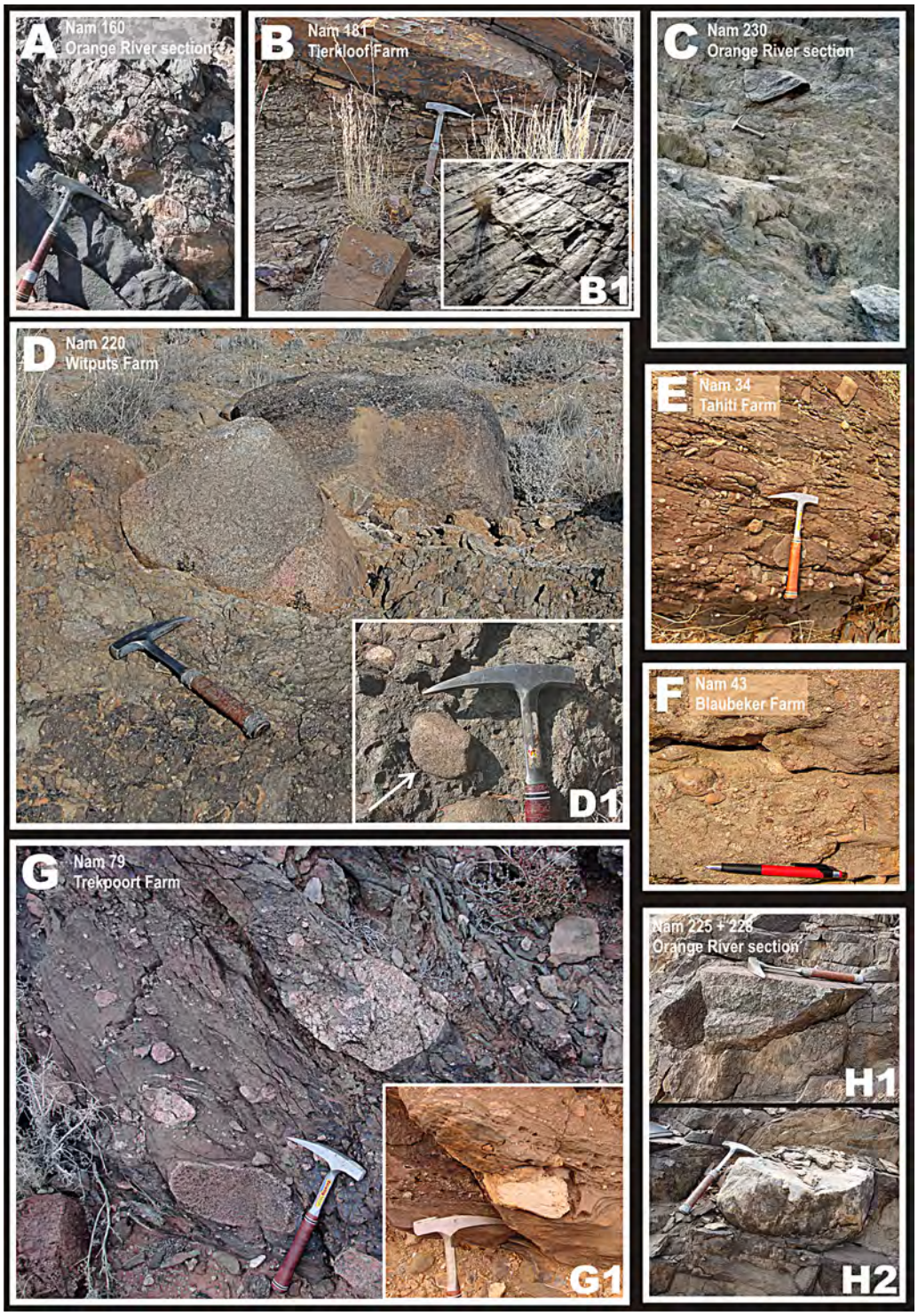

Fig. 4. Outcrop situations of all nine diamictite samples. A + B – Vingerbreek diamictite along the Orange River (road C 13, A) and from the Tierkloof Farm (B) overlying the polished and striated surface of the Kliphoek quartzite (B1), C – Numees diamictite Nam 230 along the Orange River (road C 13), D – diamictite from the Witputs Farm comprising dropstones and facetted pebbles (D1, arrow points to a facetted pebble), E + F – Blaubeker diamictite from the Tahiti Farm (E) and from the Blaubeker Farm (F), G – Numees diamictite from the Trekpoort Farm with mainly basement clasts and dropstones (G1), H – Kaigas diamictites along the Orange River (road C 13) with big boulders of quartzite (H1) and magmatic basement rocks (H2). See Fig. 3 for sample localities and Fig. 5 for stratigraphic correlation.

2.2. Trekpoort Farm

Sample Nam 79 was taken at the Trekpoort Farm at S 27°46′24.8″, E 16°38′39.2″, Alt. 871 m, ±4 m. The diamictite horizon at this point is slightly dipping towards W/SW and overlies the Wallekraal Formation that consists of the Wallekraal quartzite followed by a black siltstone that ends directly below the diamictite. It contains a large variety of pebbles and dropstones. Clasts made of basement material dominate above sedimentary ones (Fig. 4G). Fig. 4G1 shows a limestone-dropstone within the Trekpoort diamictite. Of this sample we analysed the sandy matrix.

Please cite this article in press as: Hofmann, M., et al., The four Neoproterozoic glaciations of southern Namibia and their detrital zircon record: The fingerprints of four crustal growth events during two supercontinent cycles. Precambrian Res. (2014), http://dx.doi.org/10.1016/j.precamres.2014.07.021

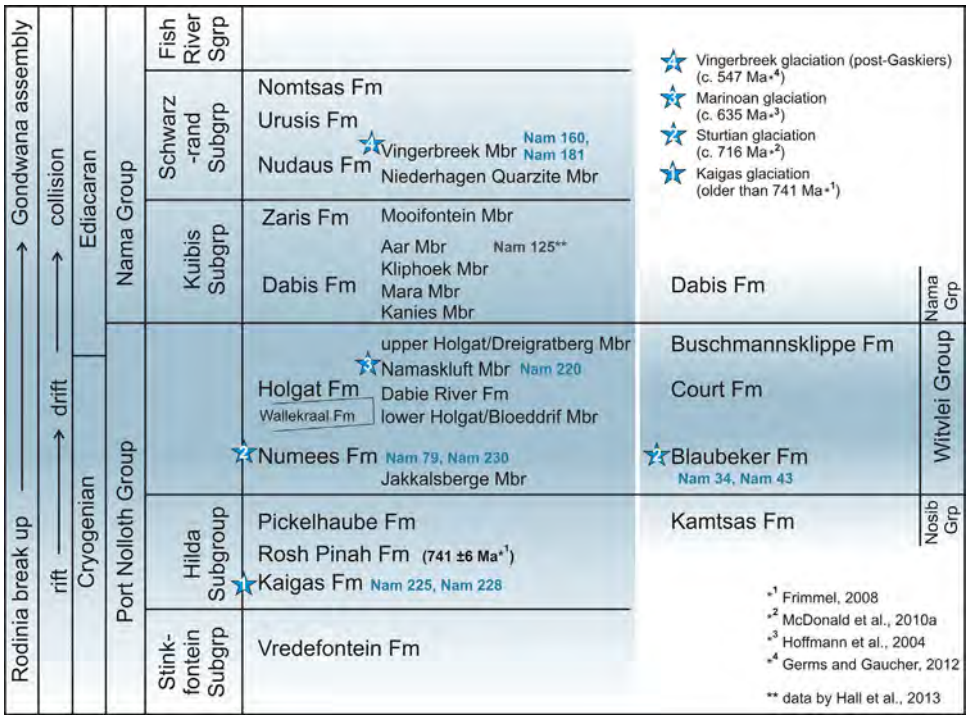

Fig. 5. Main stratigraphic units and their correlation for the study areas. The stratigraphic position of all samples is marked and correlated with four large and well-known Neoproterozoic glaciations. Stratigraphic names are based on Germs (1983), Frimmel (2008) and McDonald et al. (2010b). There is a single zircon age of c. 741 Ma (Frimmel et al., 1996; Frimmel, 2008) from the Rosh Pinah Formation giving a maximum age of sedimentation for the underlying Kaigas Formation. Sample Nam 125 (Aar Member, uppermost Dabis Formation, Aar Farm) has been taken from Hall et al. (2013).

2.3. Witputs Farm

Diamictite sample Nam 220 has been taken at the Witputs Farm at S 27°35′22.6″, E 16°41′2.9″, Alt. 993 m, ±3 m. This rock contains facetted pebbles (Fig. 4D1, arrow) and dropstones of various sizes (Fig. 4D), with most of them having a magmatic composition. The diamictite is covered by the typical yellowish-whitish-pinkish cap-carbonate of the Marinoan glaciation.

A diamictite sample from this location was also studied by Zimmermann et al. (2011). They interpreted this diamictite as non-glacial, although the presence of dropstones, facetted basement clasts (Fig. 4D1) and a cap dolomite allows another interpretation.

2.4. Tierkloof Farm

Nam 181 was collected at the Tierkloof Farm and is one of two samples of the Vingerbreek diamictite. The sample was taken at S 27°8′45.4″, E 18°12′5.4″, Alt. 1218 m, ±3 m. At this locality the Vingerbreek diamictite overlies unconformably the strongly polished and scratched surface of the Kliphoek quartzite (Fig. 4B1). Outcrops of the diamictite occur as patches of variable thickness between few cm up to max 1 m. They are covered by a sandstone layer (Fig. 4B).

2.5. Section along the Orange river

Three diamictites were sampled along the road C13 following the Orange River at its northern stream bank. The Kaigas diamictite is represented by matrix samples Nam 225 and Nam 228 from two different localities along the road. Sample Nam 225 was taken at S 28°4′47.4″, E 16°53′29.6″, Alt. 49 m, ±3 m, whereas sample Nam 228 is from S 28°5′14.9″, E 16°53′8.1″, Alt. 51 m, ±3 m. Fig. 4H1 and H2 shows big boulders of quartzite (Fig. 4H1) and magmatic basement rocks (Fig. 4H2) within the Kaigas diamictite.

A thick, foliated diamictite (Fig. 4C) that lies stratigraphically above the Kaigas formation at S 28°5′40.2″, E 16°52′54.4″, Alt. 49 m, ±3 m has been sampled as Nam 230. It is intruded by a dolerite dyke of unknown age,but most probably related to the Mesozoic opening of the Atlantic Ocean.

The second sample of the Vingerbreek diamictite matrix (Nam 160) was collected at S 28°17′45″, E 17°23′1.5″, Alt. 129 m, ±4 m. There, the Vingerbreek Member is build up by sandstones and diamictite (Fig. 4A) that unconformably overlie the Kliphoek quartzite.

3. Methods

Zircon concentrates were separated from 1–2 kg sample material at the *Senckenberg Naturhistorische Sammlungen Dresden*. After crushing the rocks in a jaw crusher, the material was sieved for the fraction between 400 and 43 μm. The heavy mineral separation was carried out by using heavy liquid LST (sodium heteropolytungstates in water) and a Frantz magnetic separator. Final selection of the zircon grains for U–Pb dating was achieved by hand-picking under a binocular microscope. Zircon grains of all grain sizes and morphological types were selected, mounted in resin blocks and polished to half their thickness. After this the zircon grains where examined regarding their Cathodoluminescence signal using an EVO 50 Zeiss Scanning Electron Microscope (*Senckenberg Naturhistorische Sammlungen Dresden*) prior to U–Pb analyses. This helps to distinguish different growth and maybe metamorphic domains within the single grains. For U–Pb analyses the laser spots where placed in domains with monophase growth patterns that show no metamorphic overprint (for some examples see Fig. 6). Zircons were analysed for U, Th, and Pb isotopes by LA-SF ICP-MS techniques at the *Senckenberg Naturhistorische Sammlungen Dresden (Museum für Mineralogie und Geologie, GeoPlasma Lab)*, using a Thermo-Scientific Element 2 XR sector field ICP-MS coupled to a New Wave UP-193

Please cite this article in press as: Hofmann, M., et al., The four Neoproterozoic glaciations of southern Namibia and their detrital zircon record: The fingerprints of four crustal growth events during two supercontinent cycles. Precambrian Res. (2014), http://dx.doi.org/10.1016/j.precamres.2014.07.021

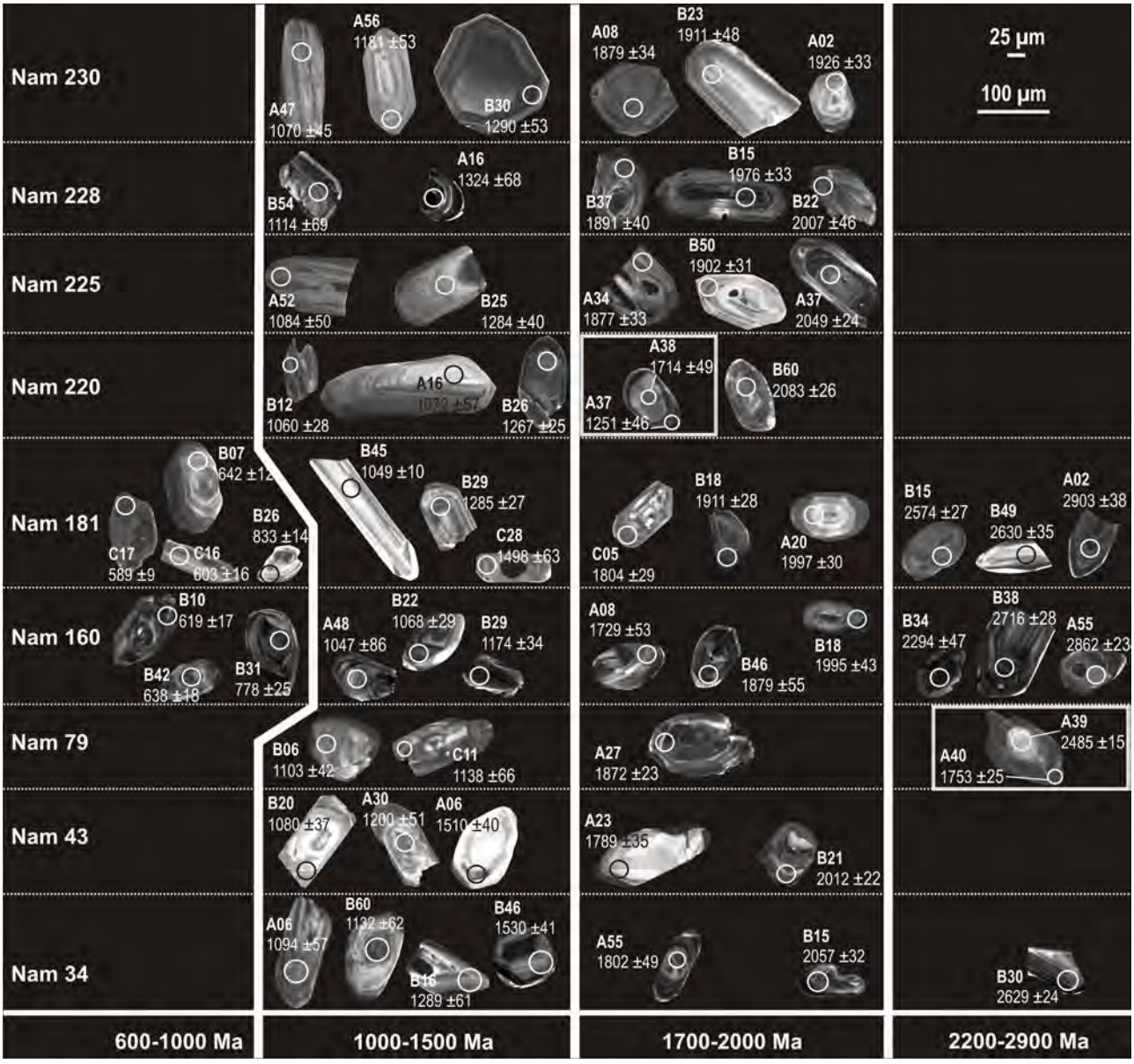

Fig. 6. Selected Cathodoluminescence pictures of zircon grains representing the main age groups for all samples. Circles indicate position of laser beam for the U–Pb analyses with a spot diameter between of 25 µm, mainly. Only zones with monophase growth patterns that show no metamorphic overprint were used for analyses. For every spot the U–Pb age is given with the 2-sigma error in Ma. Note spots A39 + A40 from sample Nam 79 and A37 + A38 from sample Nam 220, showing core and rim analyses with concordant results (see also Fig. 9).

Excimer Laser System. A teardrop-shaped, low volume laser cell (modified version of the NERC Isotope Geosciences Laboratory in UK, see Bleiner and Günther, 2001; Gerdes and Zeh, 2006, 2009) constructed by Ben Jähne (Dresden) and Axel Gerdes (Frankfurt/M.) was used to enable sequential sampling of heterogeneous grains (e.g. growth zones) during time resolved data acquisition. Each analysis consisted of approximately 15 s background acquisition followed by 20 s data acquisition, using a laser spot-size of 20–25 µm, respectively. A common-Pb correction based on the interference- and background-corrected ^{204}Pb signal and a model Pb composition (Stacey and Kramers, 1975) was carried out if necessary. The necessity of the correction is judged on whether the corrected ^{207}Pb–^{206}Pb lies outside of the internal errors of the measured ratios. Discordant analyses were generally interpreted with care. Raw data were corrected for background signal, common Pb, laser induced elemental fractionation, instrumental mass discrimination, and time-dependant elemental fractionation of Pb–Th and Pb–U using an Excel® spreadsheet programme developed by Axel Gerdes (Gerdes and Zeh, 2006; Frei and Gerdes, 2009). Reported uncertainties were propagated by quadratic addition of the external reproducibility obtained from the standard zircon GJ-1 (~0.6% and 0.5–1% for the ^{207}Pb–^{206}Pb and ^{206}Pb–^{238}U, respectively) during individual analytical sessions and the within-run precision of each analysis. Concordia diagrams (2σ error ellipses) and concordia ages (95% confidence level) were produced using Isoplot/Ex 2.49 (Ludwig, 2001) and frequency and relative probability plots using AgeDisplay (Sircombe, 2004). As for ages above 1.0 Ga the Pb–Pb ratio provides a more reliable age, this ratio was used instead of the U–Pb ratio for the following diagrams: Th–U vs Age diagram (Fig. 7) AgeDisplay diagrams (Fig. 8), and εHf (t) vs age diagram (Fig. 10). For further details on analytical protocol and data processing see Gerdes and Zeh (2006, 2009) and Frei and Gerdes (2009).

Hafnium isotope measurements were performed with a Thermo-Finnigan NEPTUNE multi collector ICP-MS at *Goethe*

Please cite this article in press as: Hofmann, M., et al., The four Neoproterozoic glaciations of southern Namibia and their detrital zircon record: The fingerprints of four crustal growth events during two supercontinent cycles. Precambrian Res. (2014), http://dx.doi.org/10.1016/j.precamres.2014.07.021

University Frankfurt (*Frankfurt/Main*) coupled to RESOlution M50 193 nm ArF Excimer (Resonetics) laser system following the method described in Gerdes and Zeh (2006, 2009). Spots of 26–40 μm in diameter were drilled with a repetition rate of 4.5–5.5 Hz and an energy density of 6 J/cm^2 during 50 s of data acquisition. The instrumental mass bias for Hf isotopes was corrected using an exponential law and a ^{179}Hf–^{177}Hf value of 0.7325. In case of Yb isotopes the mass bias was corrected using the Hf mass bias of the individual integration step multiplied by a daily βHf–βYb offset factor (Gerdes and Zeh, 2009). All data were adjusted relative to the JMC475 of ^{176}Hf–^{177}Hf ratio = 0.282160 and quoted uncertainties are quadratic additions of the within run precision of each analysis and the reproducibility of the JMC475 (2SD = 0.0028%, n = 8). Accuracy and external reproducibility of the method was verified by repeated analyses of reference zircon GJ-1 and Plesovice, which yielded a ^{176}Hf–^{177}Hf of 0.282007 ± 0.000026 (2 SD, n = 42) and 0.0282469 ± 0.000023 (n = 20), respectively. This is in perfect agreement with previously published results (e.g. Gerdes and Zeh, 2006; Slama et al., 2008) and with the LA-MC-ICP-MS long-term average of GJ-1 (0.282010 ± 0.000025; n > 800) and Plesovice (0.282483 ± 0.000025, n > 300) reference zircon at GUF.

The initial ^{176}Hf–^{177}Hf values are expressed as εHf(t), which is calculated using a decay constant value of 1.867 × 10–11 year^{-1}, CHUR after Bouvier et al. (2008) (^{176}Hf–^{177}Hf$_{CHUR,today}$ = 0.282785 and ^{176}Lu–^{177}Hf$_{CHUR,today}$ = 0.0336) and the apparent Pb–Pb ages obtained for the respective domains (table 1, electronic Supplementary material). For the calculation of Hf two stage model ages (T_{DM}) in billion years the measured ^{176}Lu–^{177}Lu of each spot (first stage = age of zircon), a value of 0.0113 for the average continental crust, and a juvenile crust ^{176}Lu–^{177}Lu$_{NC}$ = 0.0384 and ^{176}Hf–^{177}Hf$_{NC}$ = 0.283165 (average MORB; Chauvel et al., 2008) were used.

4. Results

Fig. 8 summarises the results of all U–Pb analyses for the entire sample set of this study. All analyses with a degree of concordance between 90 and 102% were regarded as "concordant" and therefore were used for diagrams and interpretative purposes. In total, 1080 laser spot measurements were done on single zircon grains. Of them 680 gave a concordant age as defined for this study. 120 zircon grains from each of the nine diamictite samples we analysed with respect to their U, Pb and Th isotope composition. The amount of concordant grains was highly variable: 77 for Nam 34, 69 for Nam 43, 63 for Nam 79, 46 for Nam 160, 66 for Nam 181, 78 for Nam 220, 98 for Nam 225, 81 for Nam 228 and 102 for Nam 230. All results concerning the U–Th–Pb isotopic composition of the zircon grains are shown in Table 1 (electronic Supplementary data) and in Figs. 7, 8 and 9.

In addition, the Hf isotope composition was analysed for selected cocordant grains of each sample (Fig. 10 and Table 2, electronic Supplementary data).

All samples yielded zircon grains with ages between c. 1.3 Ga to 1.0 Ga accompanied by a second group between c. 2.0 Ga and 1.7 Ga.

Although this is similar for all samples, the variation in the relative frequency of these ages is very important for later interpretation and correlation. Obviously there is a shift in detrital ages from older to younger sediments, starting with the two Kaigas diamictites (Nam 225 and 228) over the Sturtian diamictites (Nam 34, 43, 79 and 230), up to the Marinoan sample Nam 220 and the two post-Gaskiers Vingerbreek diamictites (Nam 160 and 181). As demonstrated in Fig. 8, the relative amount of Paleoproterozoic ages (population between 2.0 and 1.7 Ga) decreases, whereas the relative amount of Mesoproterozoic ages (age group between 1.3 and 1.0 Ga) increases steadily.

Between these two age clusters there is a gap that is only filled by some single zircon ages around 1.5 Ga occurring sporadically in some samples (e.g.: Nam 220 B27: 1557 ± 36Ma, 95% conc. or Nam 34 B46: 1530 ± 41 Ma, 102% conc., see Fig. 8).

Further, there are a few scattered zircon grains showing ages older than 2.2 Ga. The oldest U–Pb age of all analyses at 2903 ± 38 Ma (analysis A02, see Figs. 6 and 8 and Table 1, electronic Supplementary data) was found in sample Nam 181 (Vingerbreek diamictite, Tierkloof Farm).

With regard to all other samples, both of the Vingerbreek diamictites (Nam 160 and Nam 181) show a strong difference within their zircon age distribution pattern. On the one hand, they contain much younger U–Pb zircon ages (youngest grain: C17 with 598 ± 9 Ma in Nam 181) and on the other hand, they show the biggest spread of ages.

As shown in the CL images of selected zircon grains in Fig. 6 the laser spots for U–Pb analyses were put into regions with monophased growth patterns indicating magmatic origin. Therefore the obtained ages are interpreted to represent magmatic ages.

Obtained Th–U ratios are below 1.0 for a majority of 81.76% of all analysed zircon grains with concordant U–Pb age, which points to crystallisation from a felsic melt. A minority of 15 zircons (2.21%) gave values below 0.1, indicating strong metamorphic overprint. 13.38% of all analysed zircon grains (n = 91) have Th–U ratios between 1.0 and 1.5, ending up in the "transition zone" with no clear correlation to felsic or mafic melts. Only 2.65% of all analyses (n = 18) point to mafic melts as origin of the zircons (Fig. 7).

The εHf values (Fig. 10, Table 2, electronic Supplementary data) for all analysed zircon grains result in model ages that span from 1.08 Ga (Nam 181, B22) to 3.42 Ga (Nam 228 A04). Most of the analyses gave negative εHf values with a minimum at −20.0 (sample Nam 34, spot A04).

A strong mixing among the Mesoproterozoic and the Paleoproterozoic zircon ages is inferred from the wide range of possible model ages for the original crust (Fig. 10).

Mesoproterozoic zircon yielded variable εHf values between +6.8 (Nam 160, A53) and −19.7 (Nam 34, A37) with T_{DM} ages between about 2.77 Ga and 1.26 Ga. The majority of the Mesoproterozoic zircon grains gave negative εHf values. Only few of them showed positive results. The majority of these grains were found in the Vingerbreek diamictites (samples Nam 160 and 181) and some could be extracted from sample Nam 34. The highest noticed εHf value of +11.1 was achieved for zircon grain A53 from sample Nam 220 (T_{DM} 1.23 Ga).

Almost all Paleoproterozoic zircons show negative εHf values that range from 0.0 (Nam 220, A46) to −19.5 (Nam 228, A04), resulting in T_{DM} between 3.42 and 1.78 Ga.

The zircon grains with the oldest U–Pb age end up with εHf values between 0.0 (Nam 79, A39) and −6.6 (Nam 181, B32). Having model ages of 2.85–2.78 Ga they overlap the model age range obtained for the Paleoproterozoic zircons.

The youngest zircon grains of upper Neoproterozoic U–Pb age show εHf values between +3.5 (Nam 181, B22) and −5.5 (Nam 181, B06) resulting in T_{DM} ages from 1.65 to 1.08 Ga. Therefore, they plot in the same T_{DM} range as the Mesoproterozoic zircons.

5. Interpretation and discussion

Hoffmann et al. (2006) already proposed the presence of at least four temporally distinguishable glacial events in the Neoproterozoic of southern Namibia.

Please cite this article in press as: Hofmann, M., et al., The four Neoproterozoic glaciations of southern Namibia and their detrital zircon record: The fingerprints of four crustal growth events during two supercontinent cycles. Precambrian Res. (2014), http://dx.doi.org/10.1016/j.precamres.2014.07.021

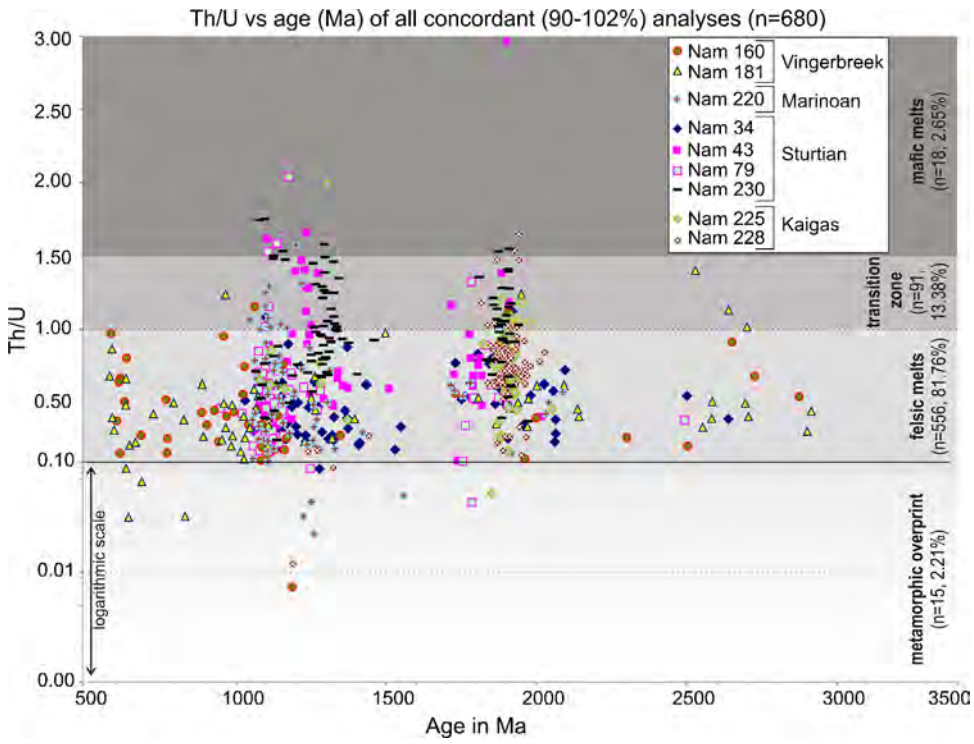

Fig. 7. Th–U versus zircon age diagram of all analyses with a degree of concordance within 90–102%, showing that the zircons in all samples were derived mainly from felsic melts (Th–U values below 1.50 and below 1.00 strict). Only a minority of 18 grains point to a mafic melt (Th–U rations above 1.50), and evidence for significant magmatic overprint (Th–U values below 0.1) is only represented by a minority of 15 single zircon grains. The diagram is based on the Th–U-ratios given in Table 1 (electronic Supplementary data).

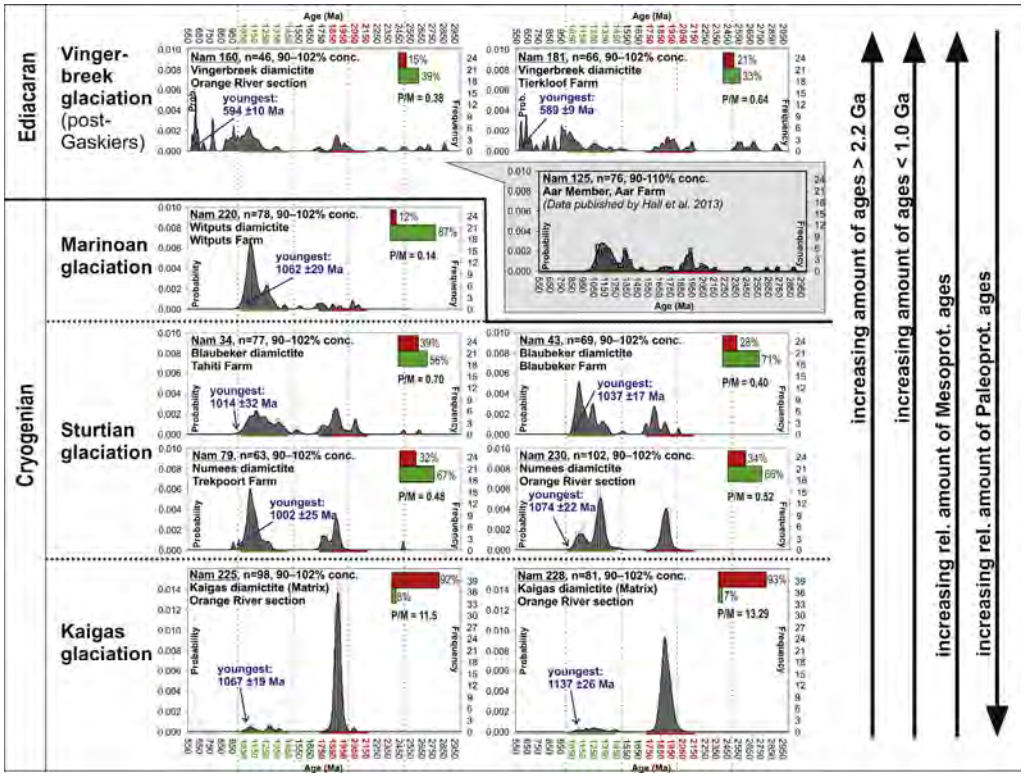

Fig. 8. Frequency vs relative probability plots using AgeDisplay (Sircombe, 2004) for all samples and their possible correlation. Note the significant shift in the absolute and relative abundance of Paleoproterozoic and Mesoproterozoic zircon ages from the Kaigas to the Vingerbreek samples. All Cryogenian samples show the same age spectra and can only be distinguished using the P/M ratio (= relative amount of Paleoproterozoic ages between 2.1 and 1.7 Ga of all concordant analyses/relative amount of Mesoproterozoic ages between 1.4 and 1.0 Ga of all concordant analyses). Results are summarised in Fig. 11. The Ediacaran post-Gaskiers Vingerbreek samples show very different zircon ages, with higher amounts of young (<1.0 Ga) and old (>2.2 Ga) ages, which allow a clear differentiation from all other samples. Diagrams are based on data given in Table 1 (electronic Supplementary data).

Please cite this article in press as: Hofmann, M., et al., The four Neoproterozoic glaciations of southern Namibia and their detrital zircon record: The fingerprints of four crustal growth events during two supercontinent cycles. Precambrian Res. (2014), http://dx.doi.org/10.1016/j.precamres.2014.07.021

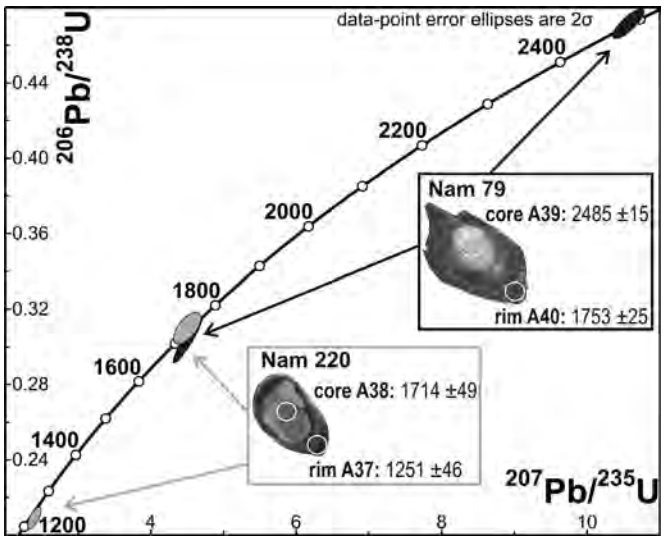

Fig. 9. Concordia diagram (2σ error ellipses) for two zircon grains showing an old core with a younger rim. These two grains reflect the thre crustal growth events from the upper Mesoproterozoic, the upper Paleoproterozoic and the lower Paleoproterozoic, which are well known from the U–Pb zircon analyses of all other samples of this study. The position of the laser spots with the resulting concordant age and 2-sigma-error in Ma is given. Scale: laser spots for sample Nam 220 and spot A40 of Nam 79: 20 μm ø, laser spot A39 of Nam 79: 25 μm ø.

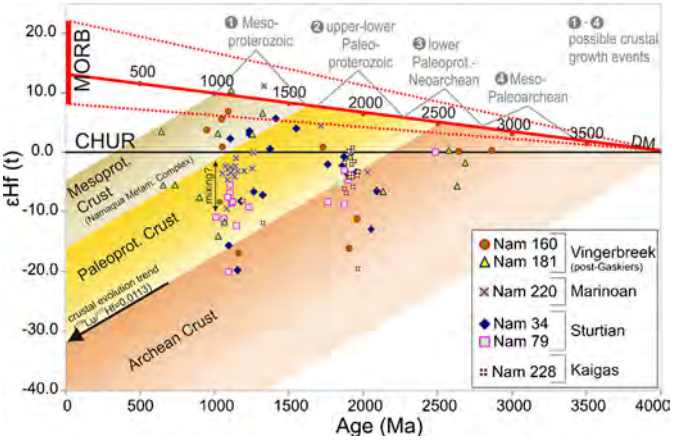

Fig. 10. εHf (t) versus age diagram of selected single zircon grains. Four events of crustal growth can be differentiated (numbers 1–4). Meso- to Paleoarchean crust was reworked during the lowermost Paleoproterozoic and during the 2.0–1.7 Ga event. The upper to lower Paleoproterozoic crust then was again recycled during the Mesoproterozoic magmatic events (1.0–1.4 Ma) and got mixed with a juvenile input given by few Mesoproterozoic analyses with positive εHf-values. The juvenile Mesoproterozoic ages were recycled during the upper Ediacaran. The data table of Lu–Hf analyses is part of the electronic Supplementary data (Table 2).

The U–Pb ages of nine analysed samples of this new study finally allow the differentiation between them by using the U–Pb detrital zircon record of the diamictites. It was possible to classify all the analysed samples and match them with four of the well-known Neoproterozoic glaciation events: Kaigas, Sturtian, Marinoan and (post-Gaskiers) Vingerbreek (Fig. 8).

Because the youngest detrital zircon grains of diamictite samples Nam 225 and 228 (Kaigas), Nam 34, 43, 79 and 230 (Sturtian) and Nam 220 (Marinoan) were all dated at c. 1.0 Ga (Fig. 8), the sediments can not be distinguished by their maximum age of sedimentation. Thus, a set up of a chronological order of the diamictites by using the youngest U–Pb-ages is impossible. Only the two samples of the Vingerbreek diamictite (Nam 160 and 181) are definitely younger, as they contain Ediacaran zircon grains, giving a maximum age of sedimentation at c. 600 Ma (Fig. 8).

For all the other samples there is a need for another distinctive feature. The most striking hint is given by the relative change of Mesoproterozoic and Paleoproterozoic ages from the Kaigas diamictites (Nam 225 and 228) over the Sturtian Numees diamictites (Nam 230, 79, 43 and 34) up to the Marinoan diamictite (Nam 220). This trend is already known from Hofmann et al. (2013) who analysed the complete Neoproterozoic section in the Namuskluft comprising strata deposited during Sturtian and Marinoan glacial events and compared these results with the diamictites from the Dreigratberg.

A differentiation between the four glacial horizons of southern Namibia can be made by the results given as summary in Fig. 11. Accordingly, a post-Gaskiers diamictite contains detrital zircons younger than 1.0 Ga, as well as older than 2.2 Ga. This is a very distinctive feature to separate this diamictite from the others. The Cryogenian diamictites do not contain any zircon grains younger than c. 1.0 Ga. Most samples also did not show grains older than 2.2 Ga (only two grains for Nam 34 and one grain for Nam 79).

We propose to distinguish the three Cryogenian diamictites by using of the P/M (= relative amount of Paleoproterozoic ages of all concordant analyses/relative amount of Mesoproterozoic ages of all concordant analyses):

$$\frac{P}{M} = \frac{\text{Paleoproterozoic}_{conc}/\text{All}_{conc}}{\text{Mesoproterozoic}_{conc}/\text{All}_{conc}}$$

The results for each sample are shown in Fig. 8, while Fig. 11 shows a summary of all P/M values of the nine diamictite samples from this study. Additionally, the six samples published by Hofmann et al. (2013) are also included into the latter one. As shown, the P/M ratios are of no use for the Ediacaran samples. But, for the Cryogenian samples, with their bimodal zircon age distribution pattern at 1.4–1.0 Ga and 2.0–1.7 Ga, the P/M seems to be a good tool for differentiation.

Based on that data we propose that Marinoan diamictites in southern Namibia show P/M values well below 0.40. The P/M ratios of Sturtian diamictites seem to be quite variable. We propose possible P/M ratios for these diamictites to be between 0.40 and 10.0. All values above 10 can be correlated with the Kaigas diamictites (see Figs. 8 and 11).

The interpretation of the Witputs diamictite (Nam 220) as being the equivalent to the upper diamictite of the Namuskluft section according to Hofmann et al. (2013) is confirmed by the overlying white-yellowish-pinkish cap-carbonate on the area of the Witputs Farm. This bright lime- or dolostone is unique for the Marinoan glaciation and points to an age of c. 635 Ma (Hoffmann et al., 2004). The samples that were interpreted as Sturtian in age (Nam 43, 43, 79 and 230) did not show a cap-carbonate on top of the diamictite that allowed a reliable correlation with the Marinoan or Sturtian glacial event. As already mentioned, in these cases, the detrital U–Pb zircon record with the P/M ratio helped to distinguish them from the younger Marinoan and the older Kaigas events.

Neoproterozoic magmatic activity is well known for this region (e.g. Richtersveld Suite, Rosh Pinah Fm., Marmora Terrane; Frimmel et al., 1996; Frimmel, 2008; Frimmel et al., 2011). The c. 741 Ma age published by Frimmel et al. (1996) derived from a rhyolite was interpreted as a syn-rift extrusive age. Remarkably, we found no zircons representing these ages in our samples except for the Vingerbreek diamictites. Nevertheless, the rocks bearing these Neoproterozoic zircons must have been at the surface and available for erosion. Following Hofmann et al. (2013), we interpret the Mesoproterozoic ages (c. 1.4–1.0 Ga) as being derived from the Namaqua Province/Namaqua Belt, which form big parts of the basement in the western and southern part of the Kalahari Craton (Fig. 1). The Paleoproterozoic ages (2.0–1.7 Ga) fit perfectly with the

Please cite this article in press as: Hofmann, M., et al., The four Neoproterozoic glaciations of southern Namibia and their detrital zircon record: The fingerprints of four crustal growth events during two supercontinent cycles. Precambrian Res. (2014), http://dx.doi.org/10.1016/j.precamres.2014.07.021

	sample	ages younger than 1.0	ages older than 2.2 Ga	conc. Paleoprot. Ages P (%)	conc. Mesoprot. Ages M (%)	P/M (= rel. abundance of conc. Mesoprot. to Paleoprot. zircons)	possible application of P/M
Vingerbreek (post-Gaskiers)	Nam 160	yes	yes	15	39	0.38	no use
	Nam 181	yes	yes	21	33	0.64	
Marinoan	Nam 70*	no	no	11	89	0.12	P/M < 0.4
	Nam 113*	no	no	26	73	0.36	
	Nam 220	no	no	12	87	0.14	
Sturtian	Nam 34	no	yes	39	56	0.70	0.4< P/M < 10
	Nam 43	no	no	28	71	0.40	
	Nam 63*	no	no	90	10	9.00	
	Nam 74*	no	no	54	46	1.17	
	Nam 79	no	yes	32	67	0.48	
	Nam 230	no	no	34	66	0.52	
	Nam 231*	no	no	41	59	0.69	
	Nam 232*	no	no	84	16	5.25	
Kaigas	Nam 225	no	no	92	8	11.50	P/M > 10
	Nam 228	no	no	93	7	13.29	

* data by Hofmann et al. (2013)

Fig. 11. Summary of U–Pb results for all diamictites from southern Namibia including analyses by Hofmann et al. (2013) and this study. To separate the Kaigas, Sturtian and Marinoan diamictites, the P/M ratios of all Cryogenian samples were calculated. Based on this data, a possible application of the P/M ratio with values below 0.4 for Marinoan diamictites, between 0.4 and 10 for Sturtian samples and above 10 for Kaigas deposits is proposed.

ages known from the Vioolsdrif Granite Suite and the Orange River Group (Frimmel, 2008; Frimmel et al., 2011), which also represents a part of the basement of the Kalahari Craton. Apart from very few grains, there is no evidence for magmatic activity in the source area of the sediments between 1.7 and 1.4 Ga, which is indicated by a significant detrital zircon age gap (Fig. 8).

Both of the Vingerbreek diamictite samples (Nam 160 and 181) contain few zircons with U–Pb ages of c. 750–700 Ma and c. 650–590 Ma. These ages are absent in all other samples from this study (see Fig. 8) and also lack in the samples from the Namuskluft and Dreigratberg sections published by Hofmann et al. (2013). Hence, we assume a change in the direction of sedimentary supply during the upper Ediacaran (Fig. 2). According to Hofmann et al. (2013) the sediment transport direction for most of the Cryogenian (throughout the Sturtian as well as the Marinoan glacial events) was from the east towards the west, transporting material directly from Kalahari Craton towards its western margin (Fig. 2).

This transport direction seems to have changed during the Ediacaran. Basin analysis (Germs, 1974, 1983) and analysis of sediments (Blanco et al., 2011) indicate a sedimentary input mainly from the east for the Kuibis and Schwarzrand Subgroups (Nama Group). A "sudden" change to a transport direction from the north started with the deposition of the uppermost Schwarzrand to lowermost Fish River Subgroup (Fig. 2). The Vingerbreek diamictite belongs to the lower Schwarzrand Subgroup. For the latter, Germs (1974, 1983) and Blanco et al. (2011) distinguish between north and south of the Osis ridge. North of the ridge the paleocurrents of the lower Schwarzrand Subgroup mainly came from the (south)east (Kalahari Craton) but also from the north and northwest, i.e. from the uplifted Damara Belt. South of Osis the contemporary sediments are inferred to have mainly been transported from the east.

We interpret the detrital material from the two Vingerbreek diamictites as the result of a western input from the Gariep Belt (see ages for Port Nolloth Zone and Marmora Terrane in Figs. 2 and 3). Thus, there was a mixed sedimentary input from the eastern Kalahari Craton, transporting typical zircon age populations of this area on the one hand (see Fig. 1), and further supply from the western Gariep Belt, as a result of tectonic activities caused by the collision of the Kalahari Craton with the Arachania terrane (e.g. Blanco et al., 2011; Hofmann et al., 2013; and references therein, Fig. 2).

This change in transport direction must have occurred after the sedimentation of the Aar Member (see stratigraphic classification in Fig. 5), because as published by Hall et al. (2013), the detrital zircon U–Pb record of the Aar Member (uppermost Dabis Formation) from the Aar Farm close to Aus in southern Namibia, does not show any zircon grains younger than c. 1.0 Ga (U–Pb zircon analyses done by M. Hofmann and U. Linnemann, *Senckenberg Naturhistorische Sammlungen Dresden, Sektion Geochronologie*, results included in Fig. 8). In fact, the sample from the Aar Member shows the same two characteristic age groups from ca 1.4 to 1.0 Ga and from 2.0 to 1.7 Ga, accompanied by some scattered older grains up to c. 2.9 Ga (Hall et al., 2013). The increase of older ages could point to ongoing unroofing events in the sediment source area. Accordingly, the Dabis Formation represents a perfect link between the detrital zircon U–Pb composition for the older sample Nam 220 (Witputz Farm) and the younger Vingerbreek diamictites (Fig. 8).

All U–Pb ages of detrital zircon grains of this study can be explained by the erosion of nearby basement units. This could result in the interpretation, that all the diamictites might represent only local debris and may not contain any information about the wider hinterland. But, the local basement in southern Namibia is characterised by a Cryogenian rifting, which is not reflected in the zircon populations of Cryogenian deposits part of our data set (Fig. 8; Hofmann et al., 2013). A local provenance would include rift-related c. 700-750 Ma old zircon ages for the Cryogenian tillites. But up to now they were only detected in the Vingerbreek Member of the late Ediacaran Nama Group (Fig. 8). For the provenance of Cryogenian sediments this points to following possibilities: (1) the sediment source was not local; debris was derived from the Kalahari Craton situated in the East, or (2) the rift related rocks were not exhumed during the Cryogenian. Frimmel (2004) published rift related zircon ages of effusive rhyolithes (c. 741 Ma) from the Port Nolloth Zone (Rosh Pina Fm.). In the case of sediment transport from western directions c. 700-750 Ma old zircons should occur in our investigated sedimentary rock. Because of the lack of such zircon ages we favour a sediment supply from the East (Kalahari Craton).

The Hf isotopic composition of the samples is similar to the ones reported by Hofmann et al. (2013) for the Namuskluft and Dreigratberg sections. Most of the zircons gave negative εHf values, pointing to potential mixing and reworking of older crust (Fig. 10).

Ediacaran and Mesoproterozoic zircon ages suggest recycling of heterogeneous crust of upper Mesoproterozoic to Neoarchaean age and most likely some mixing of the lithologies during crustal melting. The Mesoproterozoic zircon grains define the only population

Please cite this article in press as: Hofmann, M., et al., The four Neoproterozoic glaciations of southern Namibia and their detrital zircon record: The fingerprints of four crustal growth events during two supercontinent cycles. Precambrian Res. (2014), http://dx.doi.org/10.1016/j.precamres.2014.07.021

that yielded positive εHf values, pointing to a juvenile magma input from the depleted mantle during that time.

The Paleoproterozoic zircons result from recycling of a lower Paleoproterozoic to Paleoarchean crust.

The Hf isotopic composition and the εHf values (Fig. 10) allow to distinguish between four time periods of crustal growth for the western part of the Kalahari Craton: (1) The oldest event of crustal development can be traced back to the Meso- and Paleoarchean (c. 3.42–2.8 Ga). (2) A second event followed probably from the lower Paleoproterozoic to the Neoarchaean (c. 2.8–2.27 Ga), which is confirmed by most of the Hf isotope analyses obtained from the Paleoproterozoic zircon grains. (3) The majority of the Mesoproterozoic zircon grains point to recycling of a lower to upper Paleoproterozoic crust (c. 2.27–1.7 Ga). If this time range would only have been confirmed by the Mesoproterozoic zircons with negative εHf values, this "event" could just be the effect of a mixture between older crust and some Mesoproterozoic magmatic input during that time. Nevertheless, this event is also confirmed by a few c. 1.7–1.5 Ga zircon grains with positive εHf values that suggest the presence of almost juvenile melts. (4) The fourth event occurred during the Mesoproterozoic, with zircon grains yielding positive εHf values indicating emplacement of juvenile magma.

6. Conclusion/Summary

1. Southern Namibia comprises at least four Neoproterozoic diamictites that can be matched to the Kaigas, Sturtian, Marinoan and Vingerbreek (post-Gaskiers) glacial events.
2. Youngest detrital U–Pb zircon ages for all analysed sediments related to the Kaigas, Sturtian and Marinoan glacial events were at c. 1.0 Ga, making a direct correlation by maximum age of sedimentation impossible.
3. Correlation and differentiation of these glacial deposits is possible by using the complete detrital zircon U–Pb age spectra showing a significant change of the relative abundance of concordant Mesoproterozoic to Paleoproterozoic zircon ages. This P/M ratio establishes a useful tool to distinguish the Cryogenian diamictites from each other: Marinoan samples: P/M < 0.4, Sturtian samples: 0.4 < P/M < 10, Kaigas samples: P/M > 10.
4. Although the detrital zircon ages of our samples correspond to more ore less local basement, the Kaigas, Sturtian and Marinoan diamictites lack the ages of Cryogenian rifting that is well known in southern Namibia. Therefore, we assume that the sediment source area can not be local., but mainly derived from the East (Kalahari Craton).
5. The constant sedimentation lasted throughout the Cryogenian up to the late Ediacaran (represented by the deposition of the Aar Member (Dabis Formation, Kuibis Subgroup, Nama Group).
6. Sediment input from the west (Gariep Belt) occurred in the late Ediacaran Vingerbreek Member (post-Gaskiers glaciation, c. 547 Ma), which could be due to the collision of the Arachania terrane with the Kalahari Craton and the closure of the Adamastor Ocean during the Gondwana assembly. The detrital zircon record of the Vingerbreek samples show mixing of eastern and western derived detritus.
7. The Mesoproterozoic Namaqua Natal Orogeny (formation of the Namaqua Belt) is the only period showing input of juvenile magmatic material (with positive εHf zircon values), indicating crustal growth not only by recycling of older crustal fragments.
8. In total, four Archaean to Proterozoic crustal growth events are recognised in the western part of the Kalahari Craton: (1) Meso- to Paleoarchean (c. 3.42–2.8 Ga), (2) lower Paleoproterozoic to Neoarchaean (c. 2.8–2.27 Ga), (3) lower to upper Paleoproterozoic (c. 2.27–1.7 Ga) and (4) Mesoproterozoic (c. 1.6–1.0 Ga).

Acknowledgments

The authors would like to thank S. Pisarevsky (University of Western Australia, Australia), P. Vickers-Rich (Monash University, Australia), and an unknown reviewer for very constructive and helpful reviews and corrections that helped to improve the manuscript a lot.

Appendix A. Supplementary data

Supplementary material related to this article can be found, in the online version, at http://dx.doi.org/10.1016/j.precamres.2014.07.021.

References

Begg, G.C., Griffin, W.L., Natapov, L.M., O'Reilly, S.Y., Grand, S.P., O'Neill, C.J., Hronsky, J.M.A., Poudjom Djomani, Y., Swain, C.J., Deen, T., Bowden, P., 2009. The lithospheric architecture of Africa: Seismic tomography, mantle petrology, and tectonic evolution. Geosphere 5, 23–50.

Blanco, G., Germs, G.J.B., Rajesh, H.M., Chemale Jr., F., Dussin, I.A., Justino, D., 2011. Provenance and paleogeography of the Nama Group (Ediacaran to early Paleozoic, Namibia): Petrography, geochemistry and U–Pb detrital zircon geochronology. Precambrian Res. 187, 15–32.

Bleiner, D., Günther, D., 2001. Theoretical description and experimental observation of aerosol transport processes in laser ablation inductively coupled plasma mass spectrometry. J. Anal. At. Spectrom. 16, 449–456.

Bouvier, A., Vervoort, J.D., Patchett, P.J., 2008. The Lu–Hf and Sm–Nd isotopic composition of CHUR: constraints from unequilibrated chondrites and implications for the bulk composition of terrestrial planets. Earth Planet. Sci. Lett. 273, 48–57.

Bowring, S., Myrow, P., Landing, E., Ramezani, J., Grotzinger, J., 2003. Geochronological constraints on terminal Proterozoic events and the rise of the Metazoans. Geophys. Res. Abstr. (EGS, Niece) 50, 13219.

Chauvel, C., Lewin, E., Carpentier, M., Arndt, N.T., Marini, J.C., 2008. Role of recycled oreanic basalt and sediment in generating the Hf–Nd mantle array. Nat. Geosci. 1, 64–67.

Evans, A.D.E., 2009. The palaeomagnetically viable, long-lived and all-inclusive Rodinia supercontinent reconstruction. In: Murphy, J.B., Keppie, J.D., Jynes, A.J. (Eds.), Ancient Orogens and Modern Analogues. Geol. Soc. Lond. Spec. Publ. 327, 371–404.

Frei, D., Gerdes, A., 2009. Precise and accurate in situ U–Pb dating of zircon with high sample throughput by automated La-SF-ICP-MS. Chem. Geol. 261, 261–270.

Frimmel, H.E., Klötzli, U., Siegfried, P., 1996. New Pb-Pb single zircon age constraints on the timing of Neoproterozoic glaciation and continental break-up in Namibia. J. Geol. 104, 459–469.

Frimmel, H.E., 2008. Neoproterozoic Gariep Orogen. In: Miller, R. McG. (Ed.), The Geology of Namibia, Volume 2: Neoproterozoic to Lower Palaeozoic. Geological Survey, Namibia, 14-1-14-39.

Frimmel, H.E., Basei, M.S., Gaucher, C., 2011. Neoproterozoic geodynamic evolution of SW-Gondwana: a southern African perspective. Int. J. Earth Sci. (Geologische Rundschau) 100, 323–354.

Gaucher, C., Frimmel, H.E., Germs, G.J.B., 2010. Tectonic Events and Palaeogeographic Evolution of Southwestern Gondwana in the Neoproterozoic and Cambrian. In: Gaucher, C., et, al. (Eds.), Neoproterozoic-Cambrian Tectonics, Global Change and Evolution. Developments in Precambrian Geology, 16. Elsevier, Amsterdam, pp. 295–318.

Gerdes, A., Zeh, A., 2006. Combined U–Pb and Hf isotope LA-(MC-)ICP-MS analysis of detrital zircons: Comparison with SHRIMP and new constraints for the provenance and age of an Armorican metasediment in Central Germany. Earth Planet. Sci. Lett. 249, 47–61.

Gerdes, A., Zeh, A., 2009. Zircon formation versus zircon alteration – new insights from combined U–Pb and Lu–Hf in-situ La-ICP-MS analyses of Archean zircons from the Limpopo Belt. Chem. Geol. 261 (3–4), 230–243.

Germs, G.J.B., 1974. The Nama Group in South West Africa and its relationship to the Pan African Geosyncline. J. Geol. 82, 301–317.

Germs, G.J.B., 1983. Implications of a sedimentary facies and depositional environmental analysis of the Nama Group in South West Africa/Namibia. In: Miller, R. Mc. (Ed.), Evolution of the Damara Orogen of South West Africa/Namibia. Geol. Soc. S. Afr. Spec. Publ. 11, 89–114.

Germs, G.J.B., Gaucher, C., 2012. Nature and extent of a late Ediacaran (ca. 547 Ma) glaciogenic erosion surface in southern Africa. S. Afr. J. Geol. 115, 91–102.

Hall, M., Kaufmann, A.J., Vickers-Rich, P., Ivanotsov, A., Trusler, P., Linnemann, U., Hofmann, M., Elliott, D., Cui, H., Fedonkin, M., Hoffmann, K.-H., Wilson, S.A., Schneider, G., Smith, J., 2013. Stratigraphy, paleontology and geochemistry of the later Neoproterozoic Aar Member, southwest Namibia: Reflecting environmental controls on Ediacara fossil preservation during the terminal Proterozoic in African Gondwana. Precambrian Res. 238, 214–232.

Hofmann, M., Linnemann, U., Hoffmann, K.-H., Gerdes, A., Eckelmann, K., Gärtner, A., 2013. The Namuskluft and Dreigratberg sections in southern Namibia (Kalahari Craton, Gariep Belt): a geological history of Neoproterozoic rifting and recycling of cratonic crust during the dispersal of Rodinia until

the amalgamation of Gondwana. Int. J. Earth Sci. (Geologische Rundschau), http://dx.doi.org/10.1007/s00531-013-0949-6.
Hoffmann, K.-H., Condon, D.J., Bowring, S.A., Crowley, J.L., 2004. U–Pb zircon date from the Neoproterozoic Ghaub Formation, Namibia: Constraints on Marinoan glaciation. Geol. Surv. Am. 32–39, 817–820.
Hoffmann, K.H., Condon, D.J., Bowring, S.A., Prave, A.R., Fallick, A., 2006. Lithostratigraphic, carbon (d13C) isotope and U–Pb zircon age constraints on early Neoproterozoic (ca. 755 Ma) glaciation om the Gariep Belt, Southern Namibia. In: Snowball Earth Conference, Ascona, Switzerland.
Jacobs, J., Pisarevsky, S., Thomas, R.J., Becker, T., 2008. The Kalahari Craton during the assembly and dispersal of Rodinia. Precambrian Res. 160, 142–158.
Li, Z.X., Bogdanova, S.V., Collins, A.S., Davidson, A., De Waele, B., Ernst, R.E., Fitzsimons, I.C.W., Fuck, R.A., Gladkochub, D.P., Jacobs, J., Karlstrom, K.E., Lu, S., Natapov, L.M., Pease, V., Pisarevsky, S.A., Thrane, K., Vernikovsky, V., 2008. Assembly, configuration, and break-up history of Rodinia: a synthesis. Precambrian Res. 160, 179–210.
Ludwig, K.R., 2001. User's manual for Isoplot/Ex rev. 2.49. Berkeley Geochronology Center Special Publication 1a, Berkeley, pp. 56.
Mawson, D., Sprigg, R.C., 1950. Subdivision of the Adelaide System. Aust. J. Sci. 13, 69–72.
McDonald, F.A., Schmitz, M.D., Crowley, J.L., Roots, C.F., Jones, D.S., Maloof, A.C., Strauss, J.V., Cohen, P.A., Johnston, D.T., Schrag, D.P., 2010a. Calibrating the Cryogenian. Science 327, 1241–1243.
McDonald, F.A., Strauss, J.V., Rose, C.V., Dudás, F.Ö., Schrag, D.P., 2010b. Stratigraphy of the Port Nolloth Group of Namibia and South Africa and implications fort he age of Neoproterozoic iron formations. Am. J. Sci. 310, 862–888.
Pisarevsky, S.A., Wingate, T.D., Powell, C. Mc.A., Johnson, S., Evans, D.A.D., 2003. Models of Rodinia assembly and fragmentation. In: Yoshida, M., Windley, B., Dasgupta, S. (Eds.), Proterozoic East Gondwana: Supercontinent Assembly and Breakup. Geol. Soc. Lond. Spec. Publ. 206, 35–55.
Shields-Zhou, G.A., Hill, A.C., Macgabhann, B.B., 2012. The Cryogenian Period. In: Gradstein, F.M., Ogg, J.G., Schmitz, M.D., Ogg, G.M. (Eds.), The Geologic Time Scale 2012. Elsevier, pp. 393–411.
Sircombe, K.N., 2004. AgeDisplay: an Excel workbook to evaluate and display univariate geochronological data using binned frequency histograms and probability density distributions. Comput. Geosci. 30, 21–31.
Slama, J., Kosler, J., Concon, D.J., Crowley, J.L., Gerdes, A., Hanchar, J.M., Horstwood, M.S.A., Morris, G.A., Nasdala, L., Norberg, N., Schaltegger, U., Schoene, B., Tubrett, M.N., Whitehouse, M.J., 2008. Plesovice zircon – a new natural reference material for U–Pb and Hf isotopic microanalysis. Chem. Geol. 249, 1–35.
Stacey, J.S., Kramers, J.D., 1975. Approximation of terrestrial lead isotope evolution by a two-stage model. Earth Planet. Sci. Lett. 26, 207–221.
Trompette, R., 1994. Geology of Western Gondwana (2000–500 Ma). Taylor & Francis, New York, p 350.
Zimmermann, U., Tait, J., Crowley, Q.G., Pashley, V., Straathof, G., 2011. The Wiputs diamictite in southern Namibia and associated rocks: constraints for a global glaciation? Int. J. Earth Sci. (Geologische Rundschau) 100, 511–526.

Please cite this article in press as: Hofmann, M., et al., The four Neoproterozoic glaciations of southern Namibia and their detrital zircon record: The fingerprints of four crustal growth events during two supercontinent cycles. Precambrian Res. (2014), http://dx.doi.org/10.1016/j.precamres.2014.07.021